Parameters Affecting Fluid Dispersion in a Continuous Oscillatory Baffled Tube

Xiongwei Ni and Nitin E. Pereira
Dept. of Mechanical and Chemical Engineering, Heriot-Watt University, Edinburgh EH14 4AS, UK

Experimental measurements on the axial dispersion of fluid in an oscillatory baffled tube that is operated continuously were studied. Two models, the continuous stirred tank with feedback and the plug flow with axial dispersion, were used to analyze the residence-time distributions and determine the axial dispersion for this system. The effect of the density of tracer solution, the tracer injection position, and the tracer injection time on the axial dispersion was explored. It was found that the axial dispersion was sensitive to the changes in the density of tracer solution, but insensitive to the tracer injection position and injection time. A correlation linking the axial dispersion with the energy dissipation in the system both in the absence and presence of fluid oscillation was established. The Isotropic Turbulence Theory was applied, and for the first time the mixing length in the system was evaluated and compared with that of other devices.

Introduction

Mixing is at the heart of the chemical process industry, as it dominates the consideration of heat/mass transfer, reaction performance, and product uniformity. Engineers often require reactors with well-defined residence times and good fluid mixing, and seek devices that exhibit close to plug-flow behavior. Research in the past ten years has shown that periodically spaced orifice baffles along the length of a tube, coupled with a net flow superimposed with a reversing oscillatory component, give both high fluid mixing and narrow residence time distributions (Brunold et al., 1989; Dickens et al., 1989; Howes et al., 1990; Mackley and Ni, 1991, 1993). The baffle edges promote the formation of eddies, which in turn increase the radial mixing in the tube. The formation and dissipation of eddies in the oscillatory baffled flow result in significant enhancement in processes, such as heat transfer (Mackley et al., 1990; Mackley and Stonestreet, 1995), mass transfer (Hewgill et al., 1993; Ni et al., 1995a,b; Ni and Gao, 1996a), particle suspension (Mackley et al., 1993), liquid–liquid reaction (Ni and Mackley, 1993), polymerization (Ni et al., 1998, 1999), flocculation (Gao et al., 1998), and crystallization. Several dimensionless groups are commonly used to describe the oscillatory baffled flow. The oscillatory Reynolds number, Re_o, defined as

$$Re_o = \frac{d\omega x_o}{\nu} \tag{1}$$

is based on the maximum oscillatory velocity, ωx_o. The Strouhal number, St, defined as

$$St = \frac{d}{4\pi x_o}, \tag{2}$$

represents the ratio of the tube diameter to the oscillatory amplitude; the larger the St, the smaller the amplitude of oscillation. The net flow Reynolds number, Re_n, defined as

$$Re_n = \frac{du}{\nu}, \tag{3}$$

is based on the net flow of fluid down the tube, where ω is the angular frequency of oscillation (rad/s); x_o the center to peak amplitude of oscillation (m); d the tube diameter (m); ν the kinematic viscosity (m^2/s); and u is the superficial net flow velocity through the tube (m/s). The rate of the axial mixing in such a device can usually be described by a single parameter, D, the axial dispersion, and more generally an inverse Peclet number, D/uL, in a nondimensional form; here L is the distance between the injection port and a measurement location. The disadvantage of using such a dimensionless group is that it depends on the choice of L when multiple monitoring ports are involved, so obviously the longer the L, the smaller the D/uL. This has proved difficult in the interpretation of results collectively. The objectives of this work

Correspondence concerning this article should be addressed to X. Ni.

are to present a comprehensive set of residence-time distribution experiments for both net and oscillatory flows in an oscillatory baffled tube 25 m long, the first one in the UK, and to model the axial-dispersion coefficient in terms of a consistent baffle separation, L_b, that is, the inverse *cell* Peclet number, D/uL_b. In this way, the dispersion modeled is independent of the measuring location and universal to the whole system. We also established a correlation linking the mixing length with the energy dissipation in the system, and for the first time evaluated the mixing length in our device, and compared them with the traditional devices. In addition, we report the effect of the density of the tracer solution, the injection location, and the injection time on the axial dispersion.

Experimental Facilities

The continuous oscillatory baffled tube used in this work is shown in Figure 1. It consisted of 14 glass tubes, each 40 mm in diameter. The first tube was 1 meter in length, while the remaining 13 tubes were 1.5 m long. These tubes were operated vertically and connected to each other by U-bends, having an outlet for either venting or draining, as shown in Figure 1. The straight sections and bends formed a single-flow path about 25 m in length. This path provides a residence time from 7 min to 2 h for different net flow Reynolds numbers. There were 287 orifice baffles in the reactor spaced at a distance equal to 1.8 times the tube diameter. Ni and Gao (1996b) identified this as the optimal spacing in their mass-transfer study. The baffles were made of stainless steel 316 and were 38 mm in diameter with a restriction ratio of 21%. There were no baffles in the bends. Each set of baffles in the straight section was supported by two 3-mm-diameter longitudinal rods.

The net flow was provided by a liquid pump from LOWARA, and the flow rates were monitored by a flow meter. Fluid oscillation was achieved by means of a crank-piston arrangement driven by a helical geared motor through a frequency inverter. A frequency range of 0–4 Hz can be achieved, and oscillation amplitude of 0–20 mm can be obtained by adjusting the off-center positions of the crank in the fly wheel. A nonreturn valve was used in the flow inlet in order to reduce any propagation of oscillation upstream.

Tracer experiments were carried out by injecting a known amount of sodium chloride (NaCl) at any of the five injection ports, the locations of which are downstream in relation to the flow inlet (see Figure 1). To follow the changes of the tracer concentration, four Vernier conductivity probes were positioned along the length of the flow path. The zeroth conductivity probe was located 50 mm immediately above the oscillator, and was upstream with the reference to the injection ports. The purpose of this probe was to detect the migration of tracer toward the oscillator at different operational conditions; the results are not included in this article. The first, second, and third probes were situated downstream of

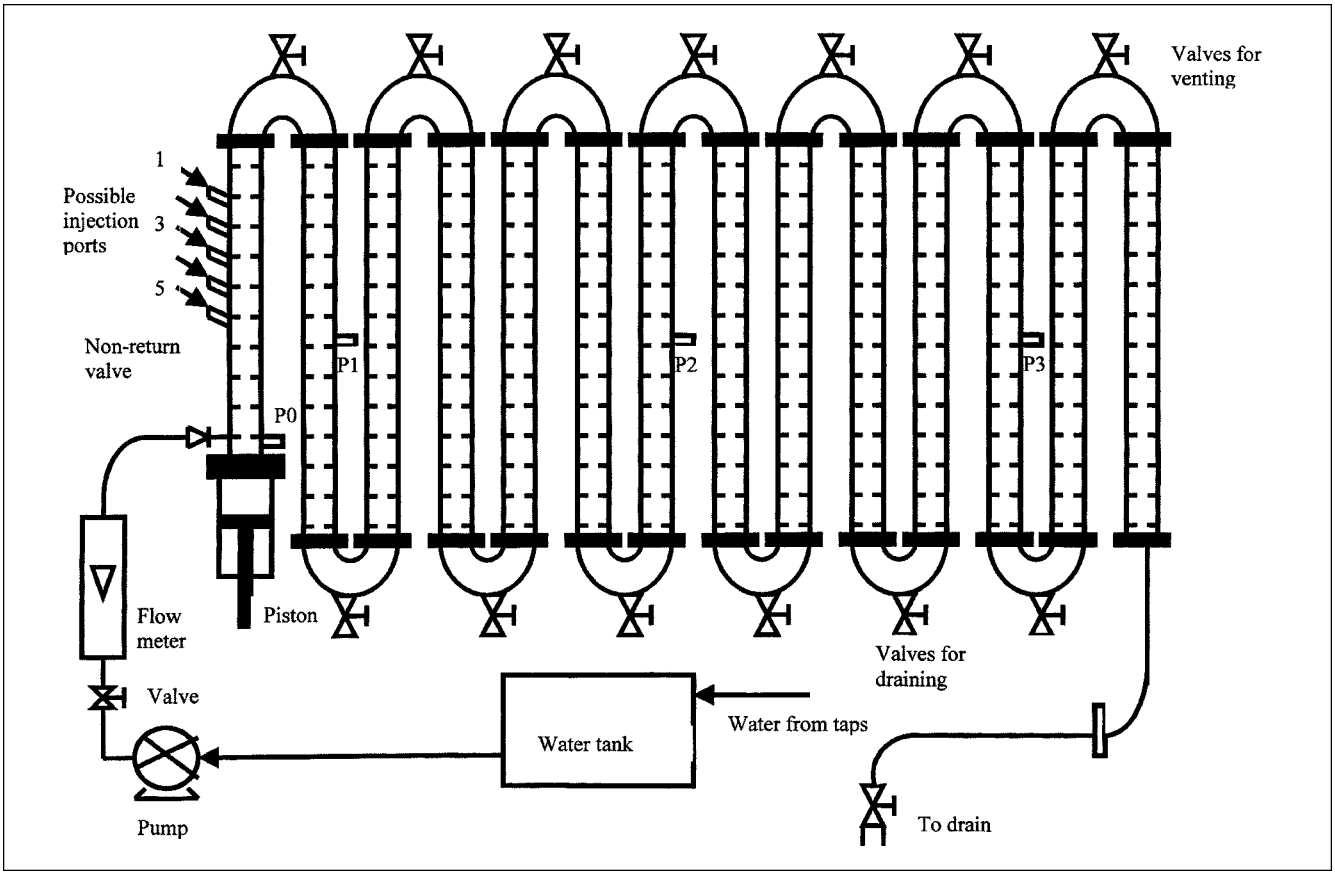

Figure 1. Continuous oscillatory baffled tube.

the tracer injection at 2.1, 11.25, and 20.6 m from the flow inlet, respectively. The signals from these probes were displayed live in both a graphic and digital form and recorded by a PC via an interface. Prior to operation, the probes were calibrated using the standard two-point method and each probe has its own calibration curve. In this article, we report our experimental measurements from probes 1–3.

In order to study the effect of tracer density on the axial dispersion, potassium nitrite (KNO_2) was used, as it has much higher solubility at room temperature compared to NaCl. We also recalibrated all the conductivity probes before the experiments.

Experimental Procedure

Twenty mL of 40 g/L NaCl tracer was injected into the system using a syringe over a known period of time downstream of the flow inlet. In all cases the process fluid was water and operated at room temperature in a one-pass fashion, that is, no recycling was made. The residence-time experiments covered oscillation frequencies from 1 Hz to 4 Hz, and the oscillation amplitudes between 0 and 8 mm, which correspond to the oscillatory Reynolds number from 0 to 8032 and the Strouhal number from ∞ to 0.4. In addition, the net flow Reynolds numbers of 0 to 2500 were also investigated.

Results

We divide our presentation into the following three categories: (1) the residence-time concentration measurements, including the tracer-density experiments from conductivity probes 1 to 3; (2) axial-dispersion modeling of such downstream concentration profiles and the evaluation of the mixing length; and (3) the effect of the tracer injection location and the injection time on the axial dispersion.

Residence-time distribution

Figure 2 shows one of the typical concentration profiles obtained at a net Reynolds number of $150 \pm 10\%$ superimposed with an oscillation amplitude of 4 mm and an oscillation frequency of 2 Hz. It can be seen that the concentration curve of probe 1 started first, as it was located nearest to the injection. This was then followed by the probes 2 and 3 at about 35 and 65 min, respectively. All the residence-time distribution (RTD) curves are well defined and essentially of a Gaussian form. Because of the low net Reynolds number, the recorded mean residence time is high, of just under 2 h for the full length of the flow path. On the increase of either the oscillation frequency from 2 to 4 Hz (Figure 3), or the oscillation amplitude from 4 to 8 mm (Figure 4), while keeping similar net flow conditions, the characteristics of the well-defined and nearly symmetrical concentration profiles are almost identical to that shown in Figure 2, and this gives clear evidence of the near plug-flow mixing that has been achieved in the device. For the conditions described in Figures 2 to 4, the concentration profiles are highly reproducible both in oscillation frequency and magnitude.

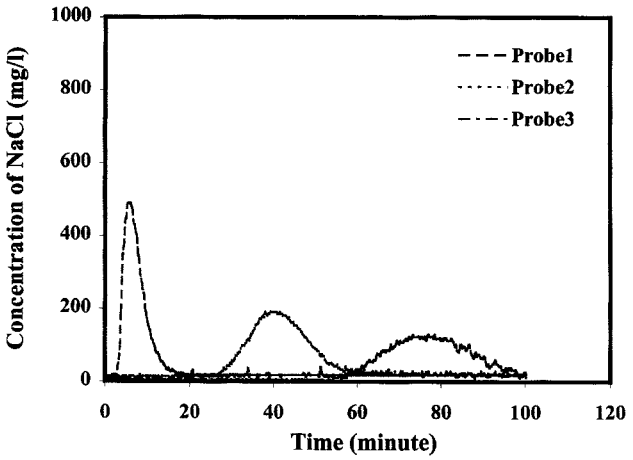

Figure 3. Concentration measurements in the oscillatory baffled tube.

$Re_n = 175$; $Re_o = 3{,}012$; 4 mm and 4 Hz; $St = 0.8$.

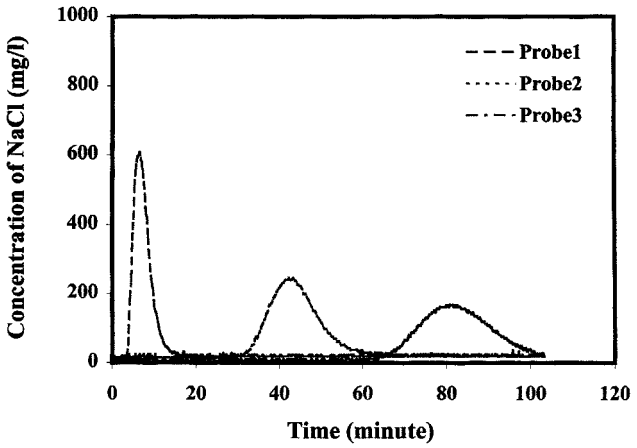

Figure 2. Concentration measurements in the oscillatory baffled tube.

$Re_n = 175$; $Re_o = 2{,}008$; 4 mm and 2 Hz; $St = 0.8$.

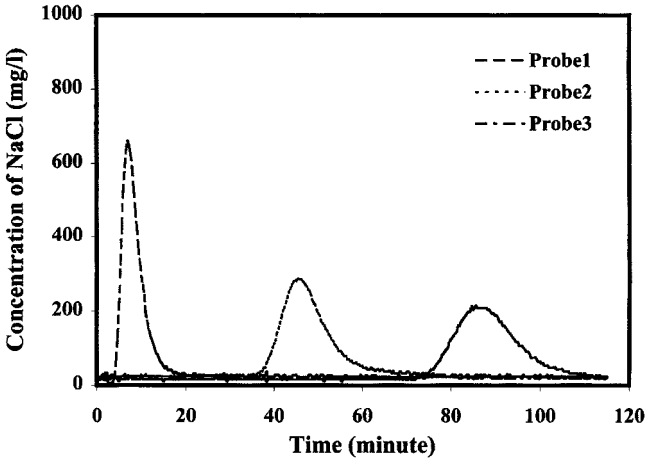

Figure 4. Concentration measurements in the oscillatory baffled tube.

$Re_n = 162$; $Re_o = 4{,}016$; 8 mm and 2 Hz; $St = 0.4$.

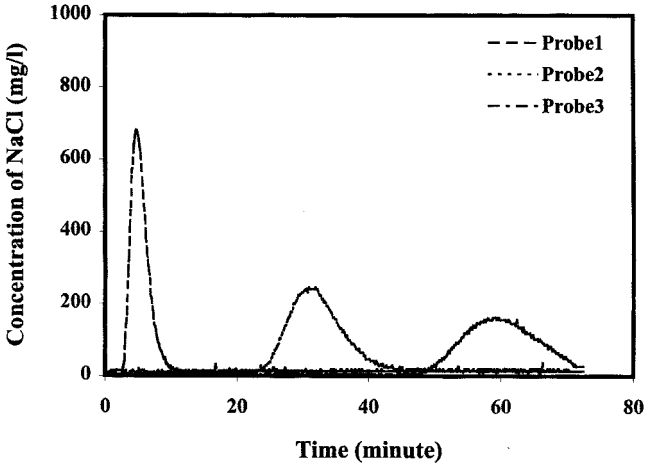

Figure 5. Concentration measurements in the oscillatory baffled tube.

$Re_n = 250$; $Re_o = 2{,}008$; 4 mm and 2 Hz; $St = 0.8$.

On the increase of the net flow Reynolds number, while keeping the oscillatory conditions unchanged, for example 4 mm and 2 Hz, the Gaussian form of the RTD curves is still clearly evident, but with reduced mean residence times, for example, from 110 min at $Re_n = 165$ to about 75 min at $Re_n = 250$ (Figure 5) and 35 minutes at $Re_n = 500$ (Figure 6). This is expected. It should be emphasized that the figures shown here are just a few samples from a large number of reproducible experiments covering a combination of the oscillation frequency of 2, 3, 4 Hz, the oscillation amplitude of 4, 6, 8 mm, and the net Reynolds number of 150, 250, 500, which corresponds to a flow rate of 0.28, 0.47, 0.95 L/min, respectively.

Dispersion Modeling. In order to understand the experimental residence-time distribution in the oscillatory baffled tube and to predict the behavior of axial dispersion, it is necessary to develop a model for the system. Several previous articles (such as Brunold et al., 1989; Dickens et al., 1989; Baird and Rama Rao, 1991) reported models for fluid dispersion and have generally used two different approaches, namely the plug flow, with axial dispersion, and the continuous stirred tank (CST) with feedback. In this article, both models were applied to our downstream concentration profiles for evaluating the fluid dispersion in the device.

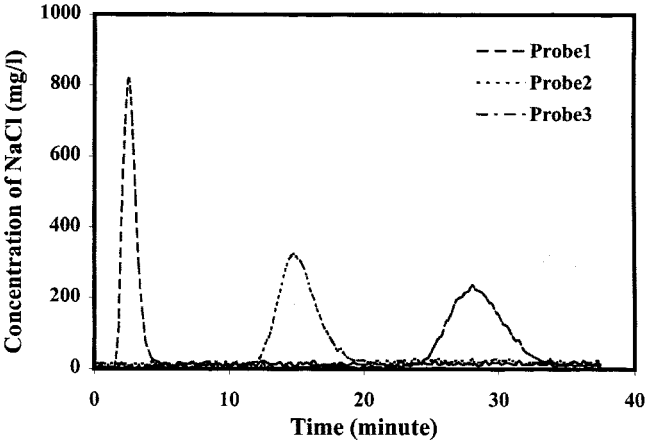

Figure 6. Concentration measurements in the oscillatory baffled tube.

$Re_n = 500$; $Re_o = 2{,}008$; 4 mm and 2 Hz; $St = 0.8$.

Plug-Flow-with-Axial-Dispersion Model. From both the previous flow visualization studies (such as Dickens et al., 1989; Mackley and Ni, 1991), and our current results, it is apparent that as a result of vortex formation and shedding in the oscillatory baffled tube, good radial mixing has been achieved, that is, the radial concentration profiles are negligible. The system can therefore be modeled as a plug-flow-with-axial-dispersion model due to eddy mixing. In this model the governing equation is

$$\frac{\partial c}{\partial t} = D\frac{\partial^2 c}{\partial x^2} - U\frac{\partial c}{\partial x}, \tag{4}$$

where c is the concentration of species (g/L); U the mean axial velocity of flow (m/s); and D the absolute axial-dispersion coefficient (m^2/s). The details of solving the preceding equation have been well documented, so we only present the numerical solution here as follows:

$$C_2(t) = C(L,t) = \int_0^t C_1(t_1)\left[\frac{u^2}{4\pi D(t-t_1)}\right]^{0.5} \times \exp\left\{-\frac{[L-U(t-t_1)]^2}{4D(t-t_1)}\right\} dt_1, \tag{5}$$

where C_1 is the tracer concentration measured upstream in relation to C_2, and t_1 is any possible injection time. To solve this convolution integral, the measured response of the first conductivity probe together with the model are used to predict the response of the second conductivity probe. The numerical program iterates to determine a best fit value for both the mean axial velocity u and the dispersion coefficient D. This process can then be repeated between the probe 2 and probe 3, and also between the probe 1 and probe 3. It should be noted that the dispersions calculated between probes 1 and 2, and between the probes 2 and 3 involved the flow along four full straight sections and five bends with a total path length of 9.25 m, while the dispersion between probes 1 and 3 covered a flow path of 18.5 m. When we apply the inverse cell Peclet number, D/uL_b, in terms of the baffle spacing to all the experimental data, the dispersion obtained is common to all the measuring locations and independent of the flow path. This gives a unified interpretation and simplifies the presentation significantly.

Figure 7 shows the inverse cell Peclet number, D/uL_b, against the oscillatory Reynolds numbers for three Strouhal numbers at a fixed net flow Reynolds number of 150. It can be seen that the axial dispersion was generally increased with the increase of the oscillatory Reynolds number for all three Strouhal numbers. Within the regime explored, D/uL_b changed by a factor of about 10. This is rather expected, since the increase in the oscillatory Reynolds number increases the power input to the system, and in turn, the turbulence, leading to more fluid dispersion. Increasing the net flow Reynolds

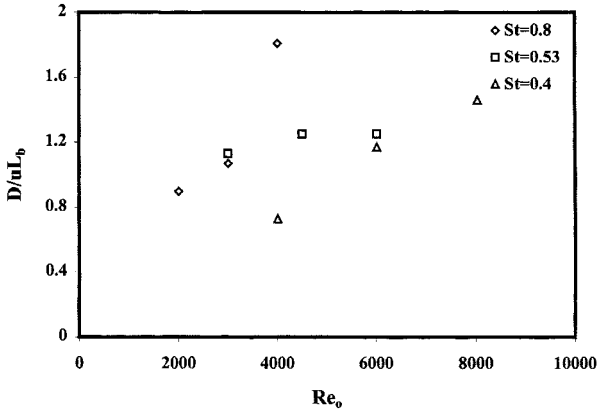

Figure 7. D/uL_b vs. oscillatory Reynolds number, Re_o, $Re_n = 150 \pm 10\%$.
Plug-flow axial dispersion model.

number from 150 to 250 (Figure 8), the flow of D/uL_b vs. Re_o is similar to that shown in Figure 7, but with smaller axial-dispersion coefficients. A further increase in the net flow Reynolds number from 250 to 500 (Figure 9) led to even more reductions in the axial-dispersion coefficients, indicating much less axial mixing at this condition. The increase in the net flow Reynolds number in a tube with baffles effectively promotes the chaotic mixing by means of eddies. Similar changes in D/uL_b for different Strouhal numbers suggest that the effect of the oscillatory motion on the axial dispersion is less sensitive at the high net flow rate. In other words, the net flow effect decouples the oscillatory effect. Overall, the axial dispersions in the given device predicted by this model are generally very low indeed, which agrees well with those that have been measured experimentally (Figures 2–6). The narrow range of the axial dispersion data further supports the evidence of the near to plug flow characteristics for this type of device.

The CST-with-Feedback Model. In the CST-with-feedback model, each interbaffled cell is represented by a perfect mixed ST, with flow to both the upstream and downstream neighboring cells. Under certain operational and geometrical conditions in the oscillatory baffled tube, each baffled cell behaves as a CST, and we have in effect a number of CST in series with feedback to and from the neighboring cells. It is therefore important to apply the CST model with feedback to evaluate the fluid dispersion in the system and compare it with that of the plug-flow-with-axial-dispersion model. For 287 baffled cells in our system, there are thus 287 CSTs in series. The identical cell Peclet number can be determined by using the algorithms from Mecklenburgh and Hartland (1975) together with the evaluations of unbiased moments from Anderssen et al. (1971).

For the discrete data points of the concentration profiles measured at probes 1, 2, and 3, the moments of area are calculated in the following way:

$$M_{i(i=0,1,2)} = \sum_{j=0}^{\infty} C_j(t) t_j^k e^{-st_j} \Delta t \qquad (k = 0,1,2), \quad (6)$$

that is, the moments are considered as the area under the concentration curve resulting from the multiplication of the distribution $C(t)$ by a weight function of $t^k e^{-st}$, suggested by Anderssen et al. (1971), where s is the optimum weighting factor. Using the unbiased-moment term proposed by Mecklenburgh and Hartland (1975) as

$$g' = \frac{\sum C_i(t) e^{-st/t_m}}{M_0}, \quad (7)$$

where t_m is the mean residence time ($= M_1/M_2$), the optimum s is the value at which g' reaches a minimum.

To characterize the dispersion in our continuous oscillatory baffled tube, the differential back-mixing method from Mecklenburgh and Hartland (1975) was used. For each value of s, the program puts $\mu = \ln(g')$ and iterates the following until the cell Peclet number, Pe, converges, where

$$Pe = \frac{uL_b}{D} = \frac{\mu^2}{\mu + s} \quad (8)$$

$$a = \sqrt{1 + \frac{4s}{Pe}} \quad (9)$$

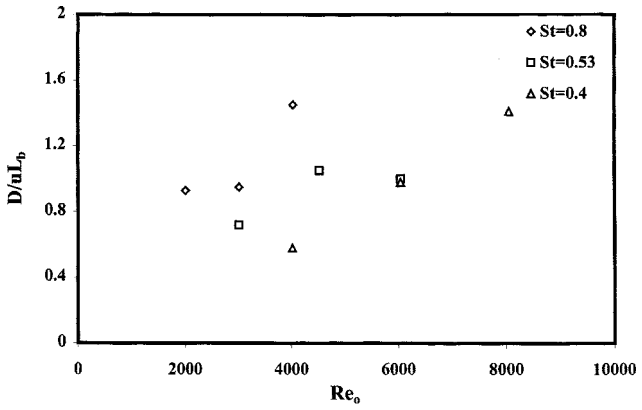

Figure 8. D/uL_b vs. oscillatory Reynolds number, Re_o, $Re_n = 250 \pm 10\%$.
Plug-flow axial dispersion model.

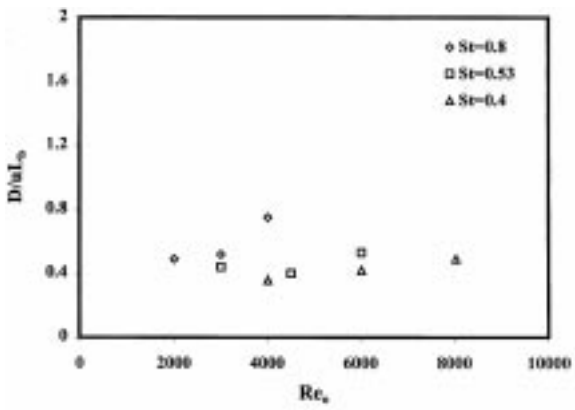

Figure 9. D/uL_b vs. oscillatory Reynolds number, Re_o, $Re_n = 500 \pm 10\%$.
Plug-flow axial dispersion model.

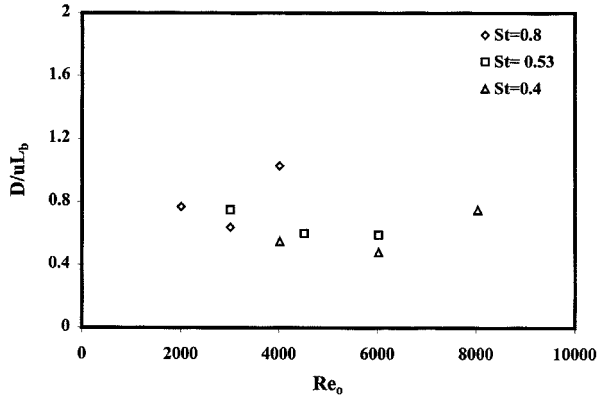

Figure 10. D/uL_b vs. oscillatory Reynolds number, Re_o, $Re_n = 150 \pm 10\%$.
CST with feedback model.

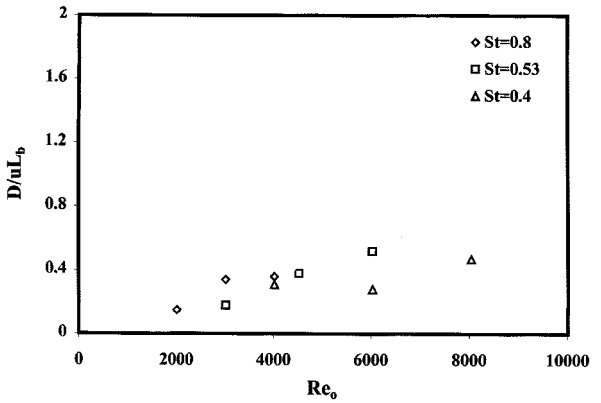

Figure 12. D/uL_b vs. oscillatory Reynolds number, Re_o, $Re_n = 500 \pm 10\%$.
CST with feedback model.

$$\mu = -\ln\left[\frac{\frac{4a}{g'} + (1-a)^2 e^{-[(1+a)Pe/2]}}{(1+a)^2}\right]. \qquad (10)$$

Figures 10–12 are the corresponding profiles to those shown in Figures 7–9 illustrating the axial dispersion coefficients calculated using the CST-with-feedback model against the oscillatory Reynolds number. We observed that the trends of the axial dispersion coefficients are less well defined with the reference to Re_o, St, as well as the net flow Reynolds number, as compared with those predicted by the plug-flow-with-axial-dispersion model. This may be due to the different mathematical iteration procedures. In general, the axial dispersions predicted by the CST-with-feedback model are smaller than that by the plug flow with the axial-dispersion model. This may be expected from the CST model, since a large number of tanks in series was used. The behavior of the given device is therefore much closer to the plug flow, and the prediction of the axial dispersion tends to be smaller. We should point out, however, that the axial dispersions in the oscillatory baffled tube predicted by both models are within the error margin and of very low value, reflecting the near-plug-flow behavior in the device. The dispersion is equivalent to that of isotropy.

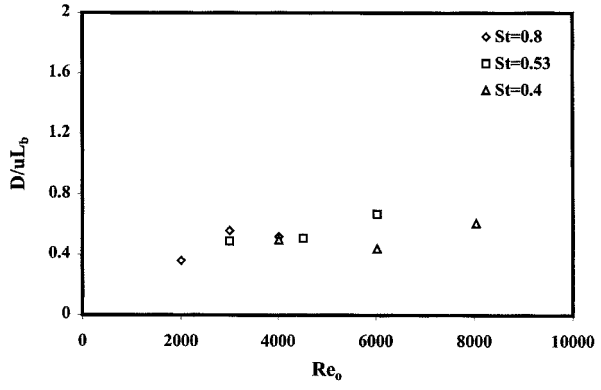

Figure 11. D/uL_b vs. oscillatory Reynolds number, Re_o, $Re_n = 250 \pm 10\%$.
CST with feedback model.

Effect of density of tracer solution on dispersion

The experimental results reported so far were obtained using a tracer solution, which is of the same density as that of the bulk liquid. Although the effect of the density gradient on mixing has been documented previously (such as Erdogan and Chatwin, 1967; Holmes et al., 1991; Aravamudan and Baird, 1996), there has been no report in relation to oscillatory baffled-tube devices. In order to understand the effect of the density of tracer solution on the axial dispersion in this device, the RTD experiments were carried out for different densities up to 1.5 times the bulk liquid with an increment of 0.1. For these experiments, potassium nitrite (KNO_2) was chosen as the tracer, since it has much higher solubility at a room temperature as compared to NaCl. The properties of the two tracers are given in Table 1.

The experiments were carried out both in the absence and presence of oscillations for three net-flow Reynolds numbers of 250, 500, and 1000, respectively. Figure 13 shows the typical concentration profile obtained at $Re_n = 250$ for a tracer concentration of 1.4 times the bulk liquid. Note that the unit of the vertical axis, the tracer concentration, is now g/L, instead of mg/L in the previous figures. It can be seen that the well-defined Guassian forms are similar to those shown in Figure 5, but with much higher magnitude of concentration. Table 2 summarizes the increased magnitudes of the tracer concentration at each probe location for each individual tracer density applied.

It is clear that the higher the density of the tracer solution, the higher the concentration responses. We applied the

Table 1. Tracer Properties

Tracer	NaCl	KNO_2
Molecular weight	35.5 g	85.1 g
Solubility (g/100 g water)	36	298
Density	2.613	1.915

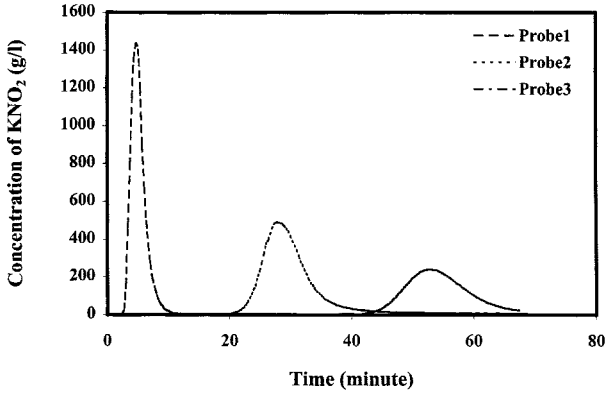

Figure 13. Concentration measurement in the oscillatory baffled tube.

Density tracer solution = 1.4; bulk fluid = water; Re_n = 250; Re_o = 2008 (4 mm and 2 Hz); St = 0.8.

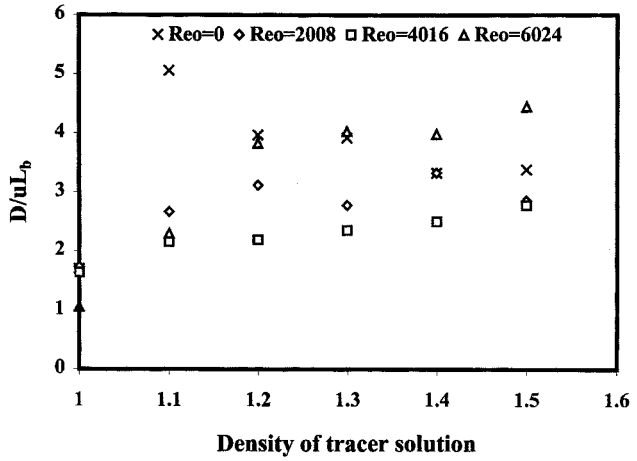

Figure 14. Effect of tracer density on D/uL_b (Re_n = 250).

plug-flow-with-axial dispersion model to the concentration profiles for different tracer solution densities to examine the effect of such density on the axial dispersion in the device. Figures 14 and 15 show the variation of D/uL_b against the density of tracer solution for the net flow Reynolds numbers of 250 and 500, respectively. It can be seen that the dispersion increased more initially at the lower densities, in particular, 1.1 and 1.2, and then seemed to level off. The trend applied to all other oscillatory Reynolds numbers examined. This experimental finding suggests that our system reacted to the density gradient rather well and dispersed the densest tracer similar to that of a specific density of 1.1. However, the initial rise between the specific densities 1.0 and 1.1 remains a mystery. In addition, we observed that when fluid oscillations were introduced to the system, the axial dispersion was reduced on average by 25% for all the dense tracer solutions investigated, as compared to that without oscillations (Figures 14 and 15). The physical interpretation of this effect is that the application of fluid oscillations in a baffled tube increases the mechanical energy (Eq. 13) to the system, which breaks up eddies and reduces the mixing length (Table 3), and thus the dispersion coefficients. This is significant, as it indicates that fluid oscillation superimposed onto a net flow through a baffled tube has a beneficial effect in reducing dispersion and in producing near-plug-flow characteristics.

Table 2. Comparison of the Magnitude of Concentration for Different Densities of Tracer Solution*

Tracer Density (ρ/ρ_w)	Probe Location		
	Conc. Probe 1 (g/L)	Conc. Probe 2 (g/L)	Conc. Probe 3 (g/L)
1.0	42.0	14.7	6.4
1.1	363.3	133.6	73.1
1.2	743.2	258.7	137.7
1.3	1,054.8	401.0	205.5
1.4	1,353.4	492.3	252.3
1.5	1,785.0	673.4	331.8

*Re_n = 250, Re_o = 2,008 (4 mm, 2 Hz), and St = 0.8.

Evaluation of Mixing Length. Applying our experimental results, the axial dispersion, D, can be used to predict the mixing length, l, in our system. The major assumption made was that viscosity plays no significant part in influencing the axial dispersion in our device. This is justified, as both the bulk fluid and the tracer solution have the viscosity of water.

We assume that the axial dispersion, D, has a power-law relationship with the density of the tracer solution, S_p, the energy dissipation per unit mass due to the presence of baffles and bends, ϵ_b, and the energy dissipation due to mechanical agitation, ϵ_m, as

$$D = n0_p^{n1}\epsilon_b^{n2}\epsilon_m^{n3}, \tag{11}$$

where

$$\epsilon_b = \frac{\Delta P u}{L_b \rho} = \frac{h_L g u}{L_b} \quad \text{(W/kg)} \tag{12}$$

$$\epsilon_m = \frac{P}{V\rho} = \frac{2N_b}{3\pi C_d^2}\frac{1-\alpha^2}{\alpha^2}x_o^3\omega^3 \quad \text{(W/kg)}, \tag{13}$$

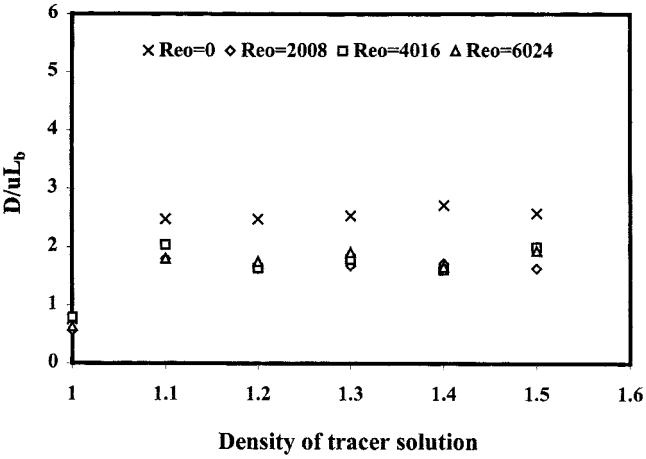

Figure 15. Effect of tracer density on D/uL_b (Re_n = 500).

Table 3. Evaluation of the Mixing Length in Our System

Re_o	Mixing Length			
	With Oscillations			
Re_n	2,008	4,016	8,032	Without Oscillations
250	14 mm	9 mm	5.4 mm	35 mm
500	16 mm	10 mm	6.3 mm	24 mm
1,000	15 mm	11 mm	7.2 mm	17 mm

where h_L is the head loss due to the presence of baffles and bends (m); N_b is the number of baffles per unit length (1/m); C_d is the orifice discharge coefficient ($= 0.7$); α is the ratio of the effective baffle orifice area to the tube area; and ρ is the fluid density (kg/m^3). From the experimental data, we obtained the values for $n0$, $n1$, $n2$, and $n3$, respectively, as

$$D = 1.8 \times 10^{-3} S_p^{0.8} \epsilon_b^{0.097} \epsilon_m^{0.0156}. \quad (14)$$

According to the Isotropic Turbulence Theory (Kolmogoroff, 1941), the dispersion relates to the mixing length and the power dissipation in a system in the following fashion:

$$D = l^{4/3} \epsilon_m^{1/3}. \quad (15)$$

Based on our axial-dispersion modeling, it is justified to assume that the dispersion achieved in our system is the same as the isotropic dispersion in Eq. 15. Thus we derived a correlation for the mixing length in our system as

$$l = 0.009 \times \left(\frac{\epsilon_b^{0.073}}{\epsilon_m^{0.24}} \right) \times S_p^{0.6}. \quad (16)$$

Knowing ϵ_b, ϵ_m, and S_p in the continuous oscillatory baffled tube the mixing length can then be evaluated over the range of experiments carried out, which is summarized in Table 3.

It can be seen that in the absence of oscillations, the mixing length varied between 43 and 87% of the column diameter over the range of the net flow Reynolds numbers studied. When the fluid oscillation is introduced the mixing length is considerably reduced, as compared with those without fluid oscillation. In addition, the mixing length decreased further with the increase of the oscillatory Reynolds numbers. This is expected as a result, as the level of agitation in the system is increased, ϵ_m increases and the mixing length decreases. The mixing length varied between 37 and 13% of the column diameter for $Re_n = 250$; 40 and 15% for $Re_n = 500$; and 37 and 18% for $Re_n = 1{,}000$. At a particular Re_o, however, the effect of the net flow has much less impact on the mixing length, and this agrees with ϵ_b having a much smaller power index than ϵ_m. This in turn suggests that the oscillatory motion strongly influences the mixing length in our system. Since the mixing length in our system varies with the oscillatory Reynolds numbers, that is, the product of oscillation frequency and amplitude, this provides the flexibility in control over the mixing length. Table 4 compares the mixing length of our system and the other existing mixing devices, and the comparison is favorable to ours.

Effect of Tracer Injection Position and Injection Time on Dispersion. The effect of the tracer injection position and the injection time on the axial dispersion in the oscillatory baffled tube were also studied for the net flow Reynolds numbers of 250 and 500, respectively, at a fixed oscillatory Reynolds number of 6024. Tracer injection ports of 1, 3, and 5, as shown in Figure 1, were used for the former experiments and the injection time of 15, 35, and 55 s were used for the latter ones. Figures 16 and 17 show the corresponding results of the axial dispersion. We can see that the axial dispersions were less sensitive to the variation of the injection positions and the injection time in our system. This is rather expected since the measuring probes were 2.1, 11.25, and 20.6 m away from the injection port. Any variations in the injection position and the injection time have been dispersed downstream, and the plug-flow characteristics in the device were achieved regardless to the injection conditions.

Table 4. Comparison of Mixing Length

Mixing System	Column Dia.	Mixing Length
Continuous OBR		
In the absence of oscillations	40 mm	(17–35) mm
In the presence of oscillations		(5.4–16) mm
Reciprocating plate column (RPC)		
Baird and Rama Rao (1991)		
In the absence of oscillations	50.8 mm	40 mm
In the presence of oscillations		3 mm
Holmes et al. (1991)		
In the absence of oscillations	76.2 mm	53 mm
In the presence of oscillations		(3.7–30) mm
Stirred-Tank Reactor		
Kawase and Moo Young (1990)	300 mm	37.5 mm
Bubble Column Reactor		
Kawase and Moo Young (1986)	230 mm	23 mm

Conclusions

We have reported that the reproducible and controlled RTDs are obtained in a continuous oscillatory baffled tube with very low axial dispersion. The axial dispersion was calculated using both the plug-flow-with-axial dispersion model and the CST-with-feedback model. We have learned that the axial-dispersion coefficient is sensitive to both the oscillation amplitude and oscillation frequency. The dispersion data suggest that the truly plug-flow behaviors dominated in the con-

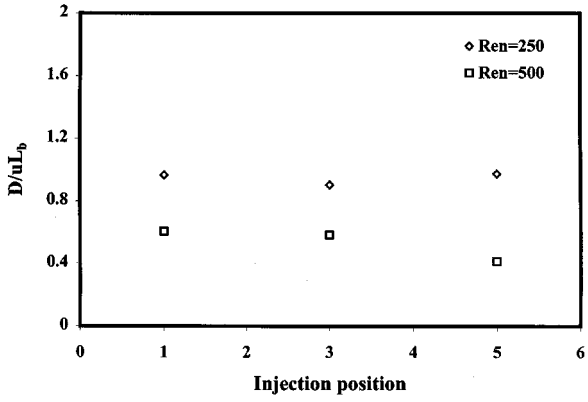

Figure 16. Effect of injection position on D/uL_b (Re_o = 6024 (8 mm and 3 Hz), St = 0.4).

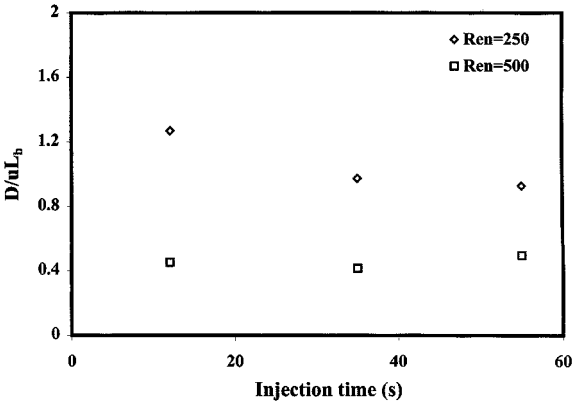

Figure 17. Effect of injection times on D/uL_b (Re_o = 6024 (8 mm and 3 Hz), St = 0.4).

tinuous oscillatory baffled tube for a range of laminar-flow net Reynolds numbers.

We have also reported that the density of the tracer solution showed a marked influence on the axial dispersion, and the axial dispersion increased with the increase in the density of tracer solution both in the absence and presence of fluid oscillation. The axial dispersion in the presence of oscillations was found to be around 25% less than that in the absence of fluid agitations. A correlation between the axial dispersion and the density of the tracer solution, as well as the energy dissipations in the system, was established, from which the mixing length in the system was evaluated. We have, for the first time, presented the range of mixing lengths under the Isotropic Turbulence Theory, which compared favorably to the existing mixing devices.

Notation

a = numerical variable
f = oscillation frequency, Hz
F = back-mixing coefficient
g = acceleration due to gravity, m/s^2
j = variable
k = constant
$n0$ = constant
P/V = power density, W/m^3
t = time variable, s
μ = numerical variable

Literature Cited

Anderssen, A. S., and E. T. White, "Parameter Estimation by the Weighted Moments Method," *Chem. Eng. Sci.*, **26**, 1203 (1971).

Aravamudan, K., and M. H. I. Baird, "Effect of Unstable Density Gradients on Back-Mixing in a Reciprocating Plate Column," *AIChE J.*, **42**, 2128 (1996).

Baird, M. H. I., and N. V. Rama Rao, "Axial Mixing in a Reciprocating Plate Column with Very Small Density Gradients," *AIChE J.*, **37**, 1019 (1991).

Brunold, C. R., J. C. B. Hunns, M. R. Mackley, and J. W. Thompson, "Experimental Observations on Flow Patterns and Energy Losses for Oscillatory Flow in Ducts Containing Sharp Edges," *Chem. Eng. Sci.*, **44**, 1227 (1989).

Dickens, A. W., M. R. Mackley, and H. R. Williams, "Experimental Residence Time Distribution Measurements for Unsteady Flow in Baffled Tubes," *Chem. Eng. Sci.*, **44**, 1471 (1989).

Erdogan, M. E., and P. C. Chatwin, "The Effects of Curvature and Buoyancy on the Laminar Dispersion of Solute in a Horizontal Tube," *J. Fluid Mech.*, **29**, 465 (1967).

Gao, S., X. Ni, R. H. Cumming, C. A. Greated, and P. I. Norman, "Experimental Investigation of Particle Flocculation in a Batch Oscillatory Baffled Reactor," *Sep. Sci. Tech.*, **33**, 2143 (1998).

Hewgill, M. R., M. R. Mackley, A. B. Pandit, and S. S. Pannu, "Enhancement of Gas-Liquid Transfer using Oscillatory Flow in a Baffled Tube," *Chem. Eng. Sci.*, **48**, 799 (1993).

Holmes, T. L., A. E. Karr, and M. H. I. Baird, "Effect of Unfavourable Continuous Phase Density Gradient on Axial Mixing," *AIChE J.*, **37**, 360 (1991).

Howes, T., and M. R. Mackley, "Experimental Axial Dispersion for Oscillatory Flow Through a Baffled Tube," *Chem. Eng. Sci.*, **45**, 1349 (1990).

Howes, T., M. R. Mackley, and E. P. L. Roberts, "The Simulation of Chaotic Mixing and Dispersion for Periodic Flows in Baffled Channels," *Chem. Eng. Sci.*, **46**, 1669 (1991).

Kawase, Y., and M. Moo-Young, "Liquid Phase Mixing in Bubble Columns with Newtonian and Non-Newtonian Fluids," *Chem. Eng. Sci.*, **41**, 1969 (1986).

Kawase, Y., and M. Moo-Young, "Mathematical Models for Design of Bioreactors: Applications of Kolmogoroff's Theory of Isotropic Turbulence," *Chem. Eng. J.*, **43**, B19 (1990).

Kolmogoroff, A. N., "The Local Structure of Turbulence in Incompressible Viscous Fluid for Very Large Reynolds Numbers," *Akad. Nauk U.S.S.R.*, **30**, 301 (1941).

Mackley, M. R., G. M. Tweddle, and I. D. Wyatt, "Experimental Heat Transfer Measurements for Pulsatile Flow in Baffled Tubes," *Chem. Eng. Sci.*, **45**, 1237 (1990).

Mackley, M. R., and X. Ni, "Mixing and Dispersion in a Baffled Tube for Steady Laminar and Pulsatile Flow," *Chem. Eng. Sci.*, **46**, 3139 (1991).

Mackley, M. R., and X. Ni, "Experimental Fluid Dispersion Measurements in Periodic Baffled Tube Arrays," *Chem. Eng. Sci.*, **48**, 3293 (1993).

Mackley, M. R., K. B. Smith, and N. P. Wise, "The Mixing and Separation of Particle Suspensions using Oscillatory Flow in Baffled Tubes," *Trans. Inst. Chem. Eng.*, **71**, 649 (1993).

Mackley, M. R., and P. Stonestreet, "Heat Transfer and Associated Energy Dissipation for Oscillatory Flow in Baffled Tubes," *Chem. Eng. Sci.*, **50**, 2211 (1995).

Mecklenburgh, J. C., and S. Hartland, *Theory of Backmixing*, Wiley, New York (1975).

Ni, X., and M. R. Mackley, "Chemical Reaction in Batch Pulsatile Flow and Stirred Tank Reactors," *Chem. Eng. J.*, **52**, 107 (1993).

Ni, X., "A Study of Fluid Dispersion in Oscillatory Flow through a Baffled Tube," *J. Chem. Technol. Biotechnol.*, **64**, 165 (1995).

Ni, X., S. Gao, R. H. Cummings, and D. W. Pritchard, "A Comparative Study of Mass Transfer in Yeast for a Batch Pulsed Baffled Bioreactor and a Stirred Tank Fermenter," *Chem. Eng. Sci.*, **50**, 2127 (1995a).

Ni, X., S. Gao, and D. W. Pritchard, "A Study of Mass Transfer in Yeast in a Pulsed Baffled Bioreactor," *Biotechnol. Bioeng.*, **45**, 165 (1995b).

Ni, X., and S. Gao, "Mass Transfer Characteristics in a Pilot Pulsed Baffled Reactor," *J. Chem. Technol. Biotechnol.*, **65**, 65 (1996a).

Ni, X., and S. Gao, "Scale Up Correlation for Mass Transfer Coefficients in Pulsed Baffled Reactors," *Chem. Eng. J.*, **63**, 157 (1996b).

Ni, X., Y. Zhang, and I. Mustafa, "An Investigation of Droplet Size and Size Distribution in Methylmethacrylate Suspensions in a Batch Oscillatory-Baffled Reactor," *Chem. Eng. Sci.*, **53**, 2903 (1998).

Ni, X., Y. Zhang, and I. Mustafa, "Correction of Polymer Particle Size with Droplet Size in Suspension Polymerisation of Methylmethacrylate in a Batch Oscillatory Baffled Reactor," *Chem. Eng. Sci.*, **54**, 841 (1999).

Manuscript received Mar. 8, 1999, and revision received Aug. 25, 1999.